Reaction Kinetics, Mechanisms and Catalysis (2019) 127:375–390
https://doi.org/10.1007/s11144-019-01534-8

Using response surface method to analyze the effect of hydrothermal post-treatment on the performance of extrudates HZSM-5 catalyst in the methanol to propylene reaction

Abolfazl Gharibi Kharaji[1,2] · Masoud Beheshti[1,3] · Jens-Uwe Repke[2] · Shahram Tangestani-nejad[4] · Oliver Görke[5] · Hamid Reza Godini[2]

Received: 6 October 2018 / Accepted: 13 January 2019 / Published online: 25 January 2019

Abstract

In this study, ZSM-5 was synthesized via the hydrothermal method and then extruded using aluminophosphate as a binder. Before using it as a catalyst in methanol to propylene reaction, it was tried to eliminate the undesired contributions of the used binder by hydrothermal post- treatment. The experimental design and the analysis of the results, especially the relation of characterization results and reactor performance, are performed by optimal response surface method in Design Expert Software. The effects of the exposing time and the temperature during the steaming procedure on the catalytic characteristics and the performance of this system were investigated for two different average particle sizes (75 and 150 μm) of this catalyst. The results of the post-treatment represent the main dependency on the catalyst particle size, where the catalyst with smaller particle size showed lower methanol conversion and selectivity towards light olefins. It was concluded that an increase in the particle size of the catalyst intensifies the transport restrictions within the zeolite structure, which consequently increases the intra-particle residence time for production of higher hydrocarbons and then facilitates their cracking in order to produce more light olefins. This needs to be taken into consideration while synthesizing the catalyst for large-scale application.

Keywords Methanol to propylene · Zeolite catalyst · Microstructure · Mesoporous structure · Steam post-treatment · Optimal response surface method

Electronic supplementary material The online version of this article (https://doi.org/10.1007/s11144-019-01534-8) contains supplementary material, which is available to authorized users.

✉ Masoud Beheshti
m.beheshti@eng.ui.ac.ir

✉ Hamid Reza Godini
hamid.r.godini@tu-berlin.de

Extended author information available on the last page of the article

Introduction

Propylene is an important intermediate chemical, which is consumed mainly for producing propylene oxide, polypropylene and acrylic acid and many other petrochemicals. Until recently, around 88% of the propylene was being obtained as the byproduct of naphtha cracking [1]. However, having considered the growing tendency for the utilization of natural gas resources for chemical production, it is predicted that the production of olefins from oil will decrease. Therefore, using an alternative on-purpose process for propylene production is necessary. Methanol-to-propylene (MTP) is an alternative promising technology through which, the already produced methanol from various sources (such as coal, natural gas, and biomass) are converted into propylene [2, 3].

In the literature, several types of zeolites have been introduced as the catalyst for the MTP process [4–6]. For industrial applications, the zeolite catalyst is generally extruded with a binder. Although the binder is primarily used to produce a desired physical shape and mechanical strength, using a binder in the catalyst structure can change the proton-exchange efficiency and physical occupation of the zeolite pores [7, 8]. The binder presence affects the porosity, diffusion and textural properties of the catalytic body, which lead to decreasing the accessibility of the gas species to the active sites [9, 10]. Therefore, it is necessary to eliminate the disadvantage of the binder existence. The hydrothermal post-treatment is a method to modify the textural properties and the structure of the catalyst. Till now, the experiments on the post-treated extrudates ZSM-5 in the catalytic application of methanol dehydration reaction are especially rare.

It is well known that the products distribution of the MTP process, as well as its catalytic lifetime, strongly depends on the zeolite framework structure, its pore architecture and acidity [2, 11]. Jabbari et al. [12] showed that increase of SiO_2/Al_2O_3 ratio leads to higher selectivity and stability of the catalyst. In the study of Ghalbi-Ahangari et al. [13] the addition of Ce decrease the surface acidity of catalyst. Liu et al. [14] partially eliminated the strong acid sites on the ZSM-5 catalyst by adding phosphorus which leads to enhancement of the propylene selectivity and catalytic lifetime. In another study, Dehertog and Froment [15] revealed that phosphorus modification led to a significant decrease in the activity of the acidic zeolite and resulted in an improved selectivity towards light olefins. Therefore, using a binder which contains phosphorus moderates the acidity of the zeolite and improves the capability of shaping it, accordingly, aluminophosphate can be considered as the binder for MTP catalyst [16]. Using mild steaming for extruded zeolite catalysts by aluminophosphate binder has one more advantage, which is the stabilization of the zeolite structure due to the reaction of the binder with the extra-framework aluminum [17–19].

In the current study, we tried to utilize the potentials of adding a promoter (phosphorous) in the structure of the binder and yet eliminate the disadvantages of the binder presence on the catalytic performance by hydrothermal post-treatment (steaming) of the catalyst. The extrudate zeolite is still not well investigated both in the change of catalyst properties during steaming and its performance

during the MTP reaction. In this context, the effects of the exposing time and temperature during the steaming procedure on the catalytic characteristics and the reaction performance of this system were investigated for two different particle sizes of the catalyst. A comprehensive investigation of the effective parameter on the steaming needs to study systematically with the least experiments and the most effective parameters. Design of experiments (DoE) is a methodology for systematically applying statistics to experimentation. Unlike OFAT (one-factor-at-a-time) which consists of varying one variable at a time while all other variables held constant, DoE provides a quick and cost-effective method for solving complex problems with many variables [20, 21].

In this paper, the effect of steaming conditions on the catalyst structure and performance was investigated in two steps. In the first step, a series of experiments were performed to determine the effective parameters and their ranges. At this step, it is tried to conducting the steaming in the conditions which have high methanol to propylene conversion, as well as an acceptable amount of olefin selectivity (the conversion rate of methanol above 80% and the selectivity of propylene greater than 30%). Next, the Optimal Response Surface Method (ORSM) is used to minimize the number of experiments and determine the main effects of the variables as well as their interactions by varying the values of all variables in parallel. The design expert software was used for designing the experiments and thereby to analyze the reactor results and recognize the effective parameters on the steaming process. In the first step, the relation between characteristic properties and the catalytic performance is assessed. In the second step, the effects of each indicated parameter on the catalytic performance are investigated in order to assess the impact of steaming conditions on the methanol conversion and olefins production in a wide range and make the results applicable for future works.

Experiments and methods

Catalyst preparation

ZSM-5 was synthesized by applying the modified hydrothermal method reported by Zhu et al. [22], where the relative ratio of materials is SiO_2: 0.0025 Al_2O_3: 0.15 TPAOH: 0.075 Na_2O: 10 H_2O. Two solutions were separately prepared in the alkaline environment (pH 11) for aluminum and silica sources. In the first solution, TPAOH and $Na_2Al_2O_4$ (as alumina source) were added and the solution was mixed for 30 min. In the second solution, SiO_2 was added and mixing was continued for 30 min. Then the second solution was added to the first one dropwise and the resulted solution was mixed for 2 h and it was then put into an autoclave for aging at 180 °C for 24 h. The produced solid was washed with distilled water and then dried at 100 °C overnight. Finally, it was calcined at 550 °C with ramp 5 K/min for 5 h. The H-form of the produced ZSM-5 was obtained by impregnating it with 1 molar NH_4NO_3 at 80 °C for 8 h followed by washing, drying and calcination at 550 °C. Then, 20 wt% aluminophosphate was added to the H-ZSM-5 according to the method described in details in Ref. [23]. The steaming procedure was carried out for catalysts particles with the mean particle size diameters

of 75 and 150 μm at the temperature range of 450–550 °C for 0–24 h. The steaming flow was 1 mL/h for 1 g of catalyst. These catalysts are denoted here as Z-S (T, t) where S, T, and t respectively refers to the average size (μm), temperature (°C) and time (h).

Catalyst characterization

Powder X-ray diffraction (XRD) patterns were conducted by a Bruker D8 Advanced diffractometer, using Co-Kα radiation (λ = 1.78897 Å, 40 kV, 35 mA) at a scanning rate of 2 °/min from scan range of 10° to 90° (2θ). The bulk composition of the prepared samples was determined by X-ray fluorescence (XRF) analyzer (BRUKER, S4 Pioneer) revealing the SiO_2/Al_2O_3 ratio. The surface textural properties and distribution of the components on the catalyst surface were determined by Zeiss Gemini Leo 1530 scanning electron microscopy (SEM) and their EDX analysis.

Nitrogen adsorption–desorption isotherms were measured by a BELSORP-mini (BEL) at − 196 °C. Before measurements, the samples were degassed at 300 °C under vacuum for 5 h. The Brunauer–Emmett–Teller (BET) equation was applied to evaluate the specific surface area. The total pore volume was derived from the nitrogen amount adsorbed at a relative pressure of 0.99. The external surface area and the micropore volume were calculated by t-plot method, while the properties of mesoporosity were derived from the BJH method.

Temperature-programmed desorption of ammonia (NH_3-TPD) was performed to determine the acidity of the samples. Before the measurements, about 100 mg of each sample was degassed at 550 °C for 2 h and then saturated with ammonia at 80 °C. After saturation, the sample was purged with helium for 30 min to remove the weakly adsorbed ammonia on the surface of the catalyst. The temperature of the sample was then raised from 80 to 550 °C at a heating rate of 10 K/min. Finally, an MS detector was used to determine the amount of the adsorbed ammonia.

Catalytic test

The catalytic activity of the catalysts for MTP was tested in a fixed-bed reactor with 8 mm inner diameter and 30 cm length. The catalysts were steamed each time at the desired conditions and then the reaction was performed at 460 °C. In all experiments, the feed was composed of an equal mass fraction of methanol and water and weight hour space velocity (WHSV) was kept at 1 h^{-1}. The product stream was analyzed by gas chromatography (Varian-3800) equipped with FID detector and HP-PLOT Q column. The product analysis was conducted after 4 h of time on stream when the composition of the products became constant and the reactor reached steady state.

Experimental design

Response Surface Method (RSM) is an empirical statistical technology that uses quantitative data obtained from appropriately designed experiments to determine regression model and operating conditions [24]. The use of RSM has been

accentuated for developing, improving and optimizing the complex processes and to evaluate the magnitude of various influencing parameters [21, 25], which has widely been applied in chemical engineering and catalysis. Optimal response surface (ORS) designs are widely used in experiments involving several factors where it is necessary to investigate the interactions effects of the factors on a response variable. ORS design is useful at the start of a response surface study where screening experiments should be performed to identify the important process or system variables. This design is often used to fit a first-order response surface model and to generate the factor effect estimation [26].

In this paper, the parameters of steaming as well as their ranges are chosen for the mild steaming. Regarding the steaming temperature, based on the results of the experiments which carried out at temperatures below 450 °C, the steaming did not make any change in the reactor results comparing to the catalyst without steaming post-treatment. At temperatures higher than 550 °C, the steaming is severe and can destroy the catalyst structure [27, 28]. With regard to the steaming time, it does not actually affect the output of the reactor at less than 3 h, and the results are similar to the catalyst without steaming post-treatment. Increasing the steaming time to more than 24 h leads to reducing the conversion of methanol and the production of propylene (the methanol conversion less than 80%, and the selectivity of propylene less than 30%). In the case of the size of the catalyst particles, they are chosen to have mass transfer resistance in the particle. The steaming for the particles below than 75 μm, significantly reduces the acidity and reduces the conversion rate (less than 80%), and increasing the particle size of the catalyst more than 150 μm do not make significant differences to of the particles with a size of 150 μm. Therefore, the range of variation for the parameters are the steaming temperature in the range of 450–550 °C, the steaming time in the range of 3–24 h and two representative particle sizes for the range of 63–88 μm (average 75 μm) and for the range of 125–177 μm (average 150 μm).The design expert software was used for designing the experiments and thereby to analyze the reactor results and recognize the effective parameters on the steaming process. In this manner, five samples were determined as case studies for investigation of three parameters in steaming. The proposed experiments by Design Expert software are shown in Table 1.

Results and discussion

Catalysts characterization

The XRD patterns for the HZSM-5 and the hydrothermally post-treated catalysts are shown in Fig. 1. The results indicate that the steaming process does not change the structure of the catalyst as ZSM-5 representative structure was continued to appear in the structure of all catalysts. Moreover, the results are in agreement with the results of previous studies [17, 19, 29, 30], which indicate the existence of phosphorus promoting the hydrothermal stability of the HZSM-5 catalyst. It was observed that the steaming conditions and the particle size are the effective parameters on the formation of $AlPO_4$ (main peak $2\Theta = 32°$) in the catalyst. As it is shown in Fig. 1,

Table 1 The proposed experiments by Design Expert software

Catalyst name	Steaming temperature (°C)	Steaming time (h)	Particle size (μm)
Z-150(550-24)	550	24	150
Z-75(550-13.5)	550	13.5	75
Z-150(450-3)	450	3	150
Z-75(450-24)	450	24	75
Z-150(500-13.5)	500	13.5	150

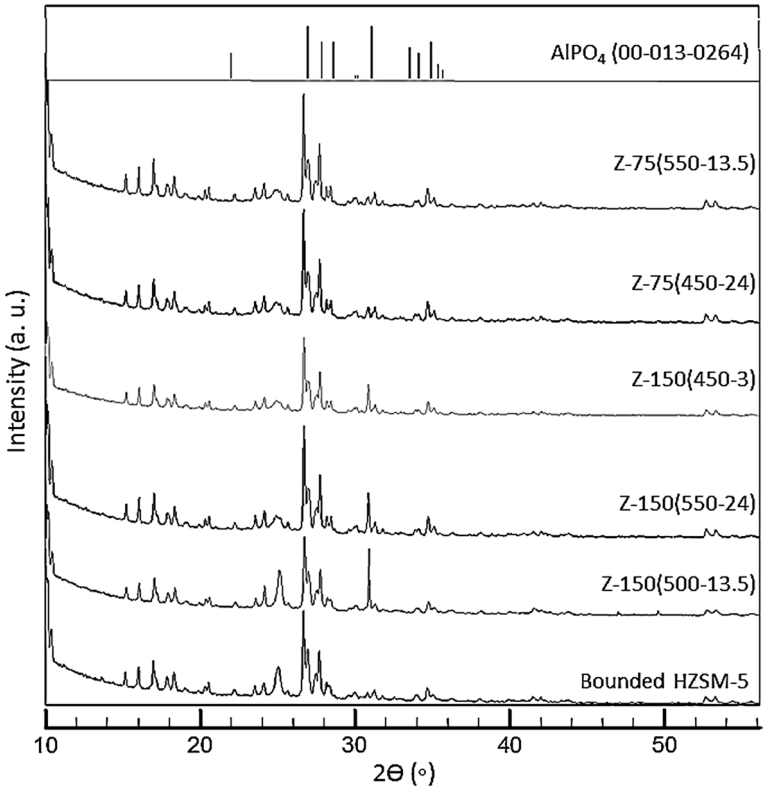

Fig. 1 The XRD patterns for the HZSM-5 and hydrothermally treated catalysts (hydrothermal condition: temperature 450, 500, and 550 °C; time: 3, 13.5, and 24 h; particle size: 75 and 150 μm)

the steaming enables $AlPO_4$ appearing in the crystal form over the larger particle size (150 μm) catalysts, where the intensity was changed by steaming condition. However, there is no crystal form $AlPO_4$ in the structure of the smaller particle size (75 μm) catalysts due to the formation of the amorphous phase and/or the good dispersion of the aluminophosphate.

The XRD results indicated the effect of particle size on the transformation of the solid phases. Therefore, in order to analyze the changes over the catalyst surface,

SEM-MAP was conducted for the catalyst particle sizes of 75 µm and 150 µm. The results are shown in Figs. 1S and 2S. In these figures, the mentioned circles indicate the existence of Al (left pictures) and P (right pictures), and the background indicate Si and O (that means the whole surface except for circles). According to the results, the dispersion of Al, P and O are very well on the surface of the smaller particle size and all of them are at the same location, therefore, these results beside the XRD results verify the good dispersion of aluminophosphate phase. The Al, P, and O elements are more concentrated at the same place on the surface of the catalyst with 150 µm particle size. According to the results, the mass transfer limitations for penetrating phosphorus into the pores of the larger particle and stronger attraction between phosphates and extra-framework aluminum [17, 30, 31] leads to the formation of $AlPO_4$ phase. It has been demonstrated that the extra-framework AlO(OH) species, which were present before phosphatation will react with the phosphorus to form an extra framework amorphous $AlPO_4$ phase [19, 32]. Hydrothermal treatment leads to crystallization of this phase as $AlPO_4$ islands [19, 32]. Therefore, the $AlPO_4$ phase appeared in the XRD patterns. The results of the nitrogen adsorption–desorption experiments are shown in Table 2.

The addition of binder decreases the specific surface area because the binder partially occupies the catalyst pore volume. Steam post-treatment has a similar effect on the specific surface area as it intensifies the thermal shrinkage of the surface. The change in BET surface area of steam post-treated catalyst is similar to the reported results of Almutairi et al. [27]. The results indicate that the steam post-treatment can have a significant impact on the specific surface area, where, these conditions affect the total pore volume and the distribution of pore diameters. Nevertheless, according to the XRD results, the catalysts structure remain stable through the steaming, while the total pore volume increases and it reaches to the higher value of extrudates ZSM-5 catalyst, therefore, increasing micropore volume at a constant structure means opening the blocked channel. According to the results shown in Table 2, the steaming recovers the micropore volume of extrudate catalyst and reaches the value of ZSM-5 particles. The similarity between micropore volume of ZSM-5 particle and those of the post-treated extrudates catalyst provides another evidence for the

Table 2 The results of the nitrogen adsorption- desorption experiments

Catalyst	$a_{s,BET}$ (m^2/g)	Micropore volume (cm^3/g)	Mesopore volume (cm^3/g)	The ratio of surface area for pore diameter 1 to 0.6 nm
HZSM-5	340	0.14	0.13	–
Extrudates HZSM-5	295	0.1	0.04	0.4
Z-150(500-13.5)	218	0.14	0.06	0.91
Z-150(550-24)	220	0.15	0.07	1.02
Z-150(450-3)	219	0.13	0.07	0.86
Z-75(450-24)	217	0.15	0.06	1.42
Z-75(550-13.5)	216	0.15	0.05	1.34

migration of the binder into the structure of the catalyst during steaming and thereby reducing the number of the blocked channel through steaming. The pore size distribution measured by the t-plot and BJH methods for micro and mesoporous are shown in Figs. 2 and 3S, respectively.

According to the results, the extrudate catalyst without steam post-treatment has a micro-mesostructure and after steaming it converts to a microporous structure with higher pore diameter. The steaming conditions change the area distribution for pore sizes of 0.6 and 1 nm (Fig. 2). To clarify this effect, the ratios of surface area for pore diameter 1 to 0.6 nm are calculated as shown in Table 2. According to the results, the catalyst particle size is a very effective parameter regarding its impact on the surface area distribution so that the catalyst with lower particle size has the higher surface distribution of 1 nm pore diameter.

The results of the surface acidity and the Si/Al ratio are shown in Table 3.

The steaming significantly affects the catalyst acidity and the Si/Al ratio. This is more pronounced for the smaller particle size catalyst, especially for long time steaming (24 h). As seen in these reported results, dealumination has occurred during the steaming and the acidity is decreased by increasing the Si/Al ratio. For the smaller particle size, the number of weak acid sites is not as much affected by the steam treatment as the number of strong acid sites. This is in agreement with the reported trends in literature for a similar system [19, 29, 33, 34].

Although the steaming conditions are not the dominant factors contributing to the observed change in the acidity of the larger particle size, the steaming post-treatment however, transforms the strong acidity to the weak one and thereby enables the formation of a new type of weak acid site [19]. According to the XRD and SEM

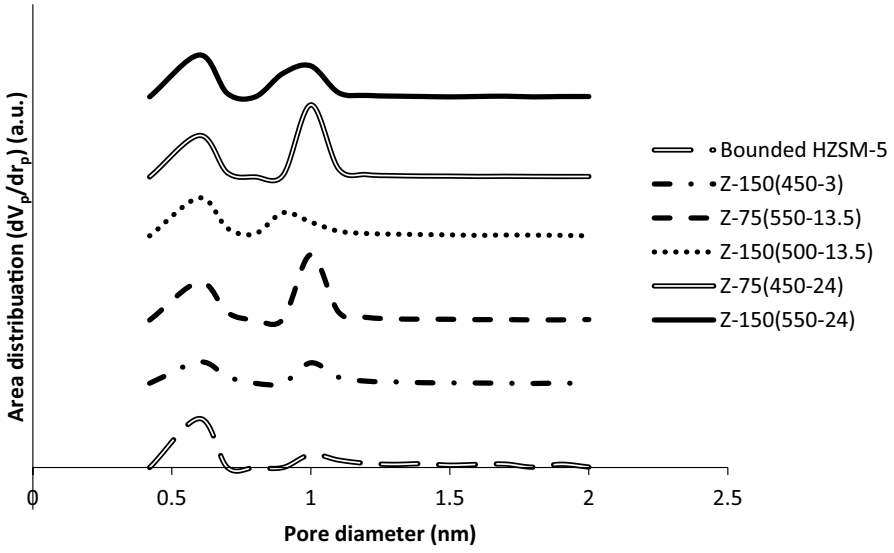

Fig. 2 The area distribution versus pore diameter according to t-plot method for the HZSM-5 and hydrothermally treated catalysts (hydrothermal condition: temperature 450, 500, and 550 °C; time: 3, 13.5, and 24 h; particle size: 75 and 150 μm)

Table 3 The results of the surface acidity and Si/Al ratio

Catalyst	Acidity, mmolNH_3/g		Si/Al
	Weak	Strong	
Extrudates HZSM-5	0.11	0.23	180
Z-150(500-13.5)	0.19	0.13	192
Z-150(550-24)	0.2	0.1	190
Z-150(450-3)	0.18	0.12	191
Z-75(450-24)	0.1	0.06	218
Z-75(550-13.5)	0.12	0.09	216

characterization results of the structure of larger particle size, it can be observed that the $AlPO_4$ is established during the steaming and the steaming conditions have less impact on the Si/Al ratio (Table 3) and thereby on the catalyst acidity. This indicates that the phosphorus either inhibits the migration of aluminium species or prevents dealumination altogether for larger particles [17, 18, 29, 30]. Therefore, the presence of the $AlPO_4$ crystalline phase results in a more stable aluminum in the catalyst.

Experiments design and statistical analysis

The proposed catalysts by design expert software (Table 1) were synthesized and the results are presented in Table 4. To validate the predicted results of experimental design, the catalysts with 8 h steaming time and 500 °C steaming temperature were synthesized for both particle sizes (75 and 150 μm), and the results also are shown in Table 4. The equations describe propylene and ethylene yields (Y_{Pr} and Y_{Et}) are shown in Table 1S. The results indicate that predicted ethylene and propylene yields are in good agreement with the actual experimental data. A first order equation is fitted to the results of propylene and ethylene yields, and their analyses of variance (ANOVA) are illustrated in Tables 2S and 3S, respectively. P values less than 0.05

Table 4 The observed and predicted propylene and ethylene yields (feed: 50 wt% methanol in water, WHSV: 1 h^{-1}, reactor temperature: 460 °C)

Catalyst	Observed propylene yield %	Predicted propylene yield %	Observed ethylene yield %	Predicted ethylene yield %
Extrudates HZSM-5	30	–	10	–
Z-150(500-13.5)	49	46.9	21	22.1
Z-150(550-24)	50	47.7	25	24.2
Z-150(450-3)	45	46.0	20	20.0
Z-75(450-24)	38	35.0	13	12.7
Z-75(550-13.5)	41	40.3	16	16.6
Z-150(500-8)	50	49.1	24	22.8
Z-75(500-8)	38	38.8	13	14.6

indicated high significant regression at 95% confidence level, and also the larger F-values results in significant model and well predicted coefficients [35]. The results given in Tables 2S and 3S showed that this regression was statistically significant. The products distribution and carbon balance of prepared catalysts and commercial catalyst are shown in Table 4S. According to the results, catalyst with larger particle size has similar reactor performance to of commercial one. The carbon balances of all experiments were higher than 90%. Therefore, the accuracy of the results are acceptable.

Effect of process variables

The methanol conversions for both particle sizes are shown in Fig. 3. The catalyst with smaller size shows the lower conversion where after being hydrothermal treated at a higher temperature and for a longer time up to 15 h, the methanol conversion increases. The methanol conversion is decreased for steaming time higher than 15 h for all temperatures. The observed trends in methanol conversion can be explained by the TPD results, so that increasing steaming time decreases the total and strong acid sites of the smaller particle catalyst and cause to decreasing methanol conversion. The results of the methanol conversion observed for the larger particle size indicate that the impact of steaming time on the methanol conversion is higher than the impact of the temperature, such that the temperature over 500 °C has no significant impact on the methanol conversion. The observed difference in the methanol conversion of the catalyst with the small and large particle sizes, as represented in Fig. 3, is due to the change in the structure and acidity of the catalysts during the steaming process. The BET results showed that the change in the catalyst structure during the steaming process depends on the catalyst particle size, so that the smaller particle size has the higher ratio of pore diameter 1 to 0.6 nm (Table 2). Therefore, in the catalyst with smaller particle size there is more accessibility to the active site yet the TPD results showing lower acidity. The catalyst with larger particle size has more methanol conversion. Therefore, it does not seems that any limitation on the accessibility of reactants to the active sites plays a significant role, therefore, in this case the methanol conversion is controlled by the acidity of the catalyst.

The trends of "propylene + ethylene" (light olefins) yields versus time and temperature of steaming for both catalyst sizes are shown in Fig. 4.

Although the particle size has no significant impact on the propylene yield (As shown in Fig. 4S), it has more influence on the ethylene and heavy olefins production (C_5, C_6 and C_{6+}). The amount of produced light olefins for the catalyst with larger particle size is more than the one generated using the smaller particle size. Although the steaming conditions have significant impacts on the light olefins yield of the catalyst with larger particles, it has less effect on the light olefins yield of the smaller one. The light olefin (C2 + C3) yields was increased from 58% for 75 µm ZSM-5 catalyst particle size to 78% for 150 µm ZSM-5 catalyst particle size at the same conditions of steaming (ST: 550 °C, St: 12 h), where the highest reported light olefins yield are around 75–80% [36–39]. Therefore, the particle size plays an important role in tailoring the product distribution and providing the maximum light

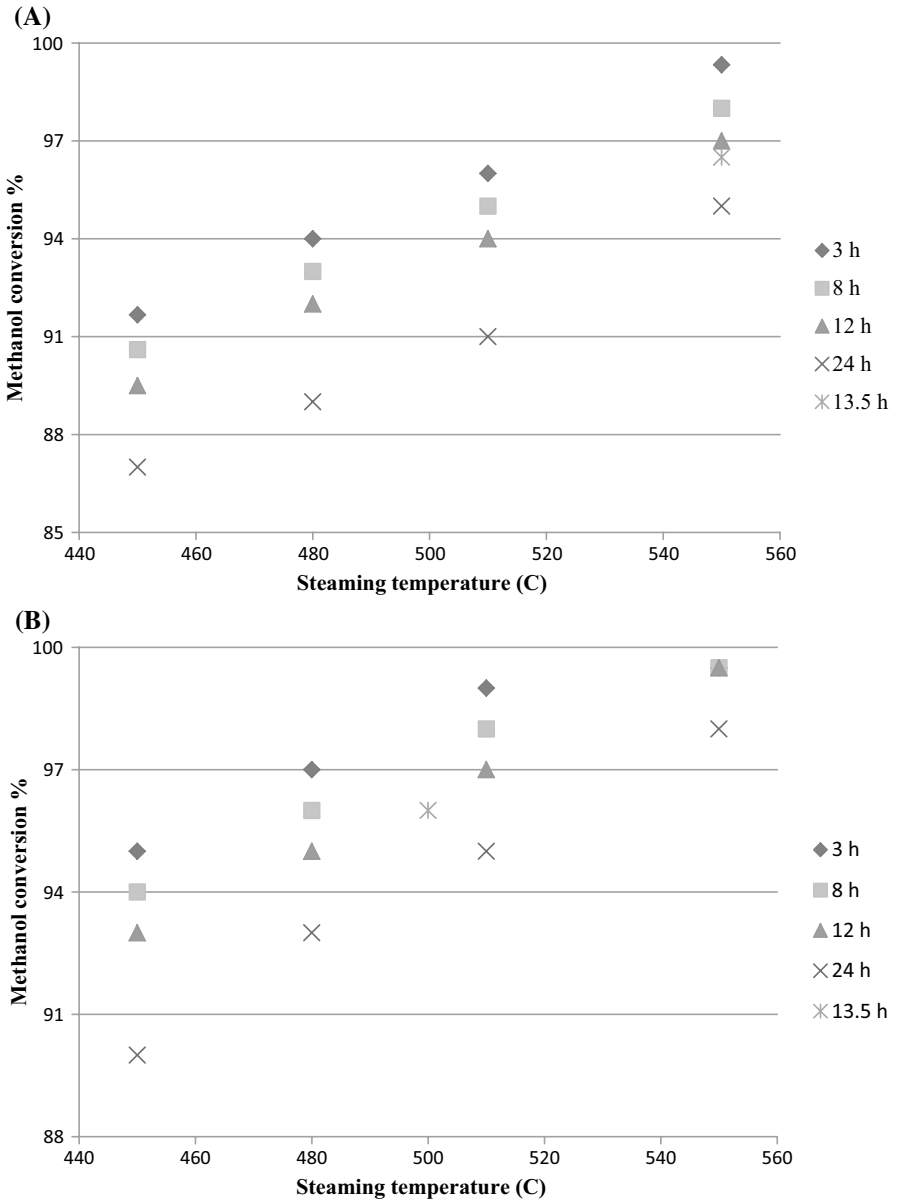

Fig. 3 The methanol conversion for the catalysts with average particle sizes **a** 75, and **b** 150 µm versus steaming time and temperature (feed: 50 wt% methanol in water, WHSV: 1 h^{-1}, Reactor temperature: 460 °C)

olefins yield. The observed results in terms of the light olefin yields are in agreement with the reported results in several previous studies [40–43]. Sugimoto et al. [40] have reported that the light olefins selectivity has been increased by increasing

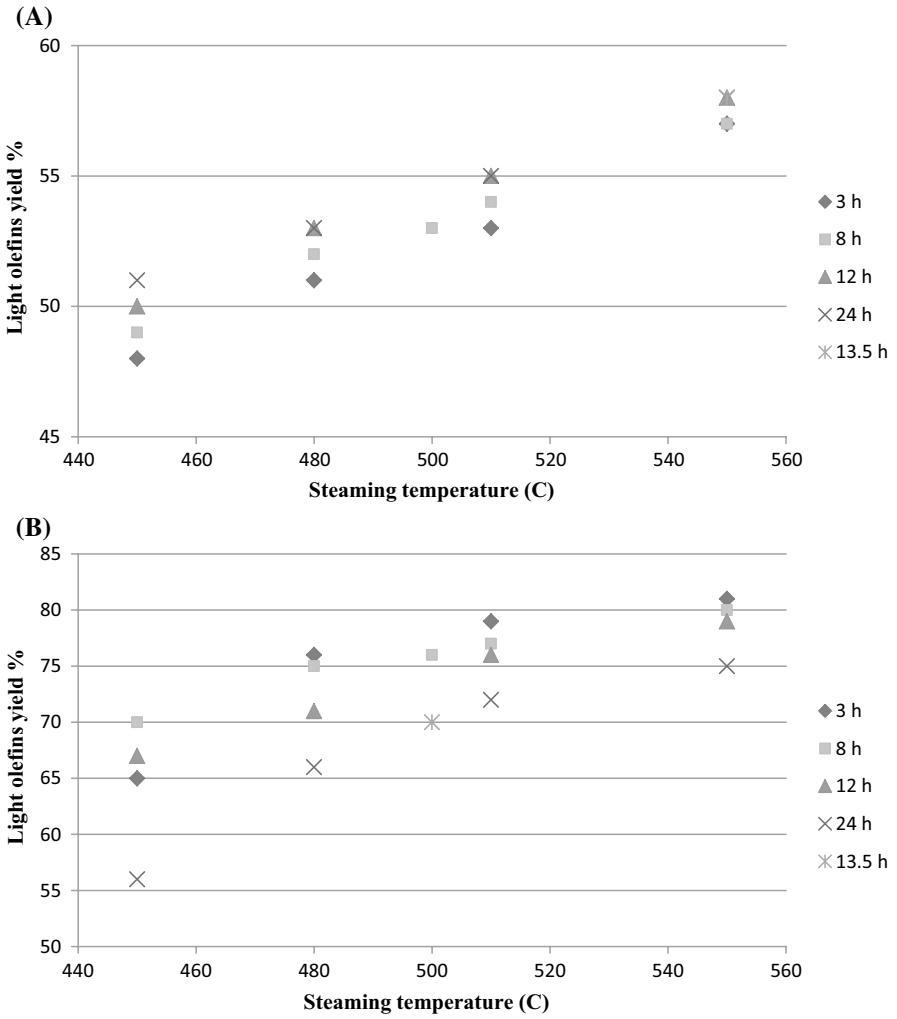

Fig. 4 Light olefins yield for the catalysts with average particle sizes **a** 75, and **b** 150 µm versus steaming time and temperature (feed: 50 wt% methanol in water, WHSV: 1 h^{-1}, reactor temperature: 460 °C)

the particle size where the effect of particle size on the ethylene selectivity has shown to be more significant. The results of Rownaghi et al. [41, 42] indicated that ethylene selectivity is higher for the catalysts with larger particle size. Khare et al. [44] showed that the selectivity towards C_2 increases monotonically while that of C_4–C_7 hydrocarbons decreases with increasing the crystallite size. The observed increase in the light olefin selectivity in this study is attributed to the improved product shape selectivity of the catalyst and the addition of $AlPO_4$ phase in the structure of larger particle size during steaming, which affects the diffusion characteristics by decreasing the pore dimensions and openings. This particularly led to longer diffusion pathways for reactants and products [45, 46] and provide the conditions for

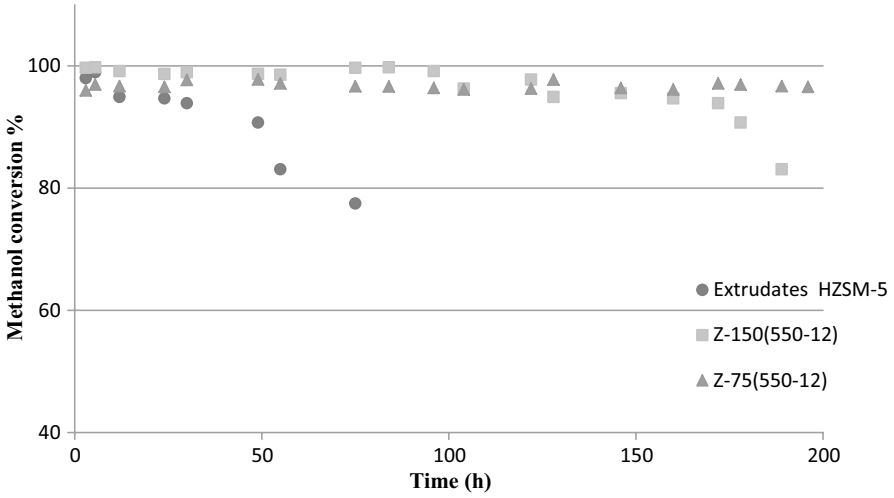

Fig. 5 Time on stream analysis of extrudates HZSM-5, Z-150(550-12) and Z-75(550-12) catalysts (feed: 50 wt% methanol in water, WHSV: 1 h^{-1}, reactor temperature: 460 °C)

multiple methylations and consequently cracking of higher hydrocarbons before exiting the catalyst. As a result, the amount of light olefins, unlike the higher ones, is reduced. Moreover, the steaming post-treatment transforms the strong acidity to the weak one, which has a positive effect on the light olefins production.

Time on stream analysis

The time on stream analysis was conducted for three samples of catalyst and the results are shown in Fig. 5. One of the samples is the catalyst without steam post-treatment and others are the post-treated catalysts with 75 and 150 µm particle sizes at 12 h of steaming time and 550 °C of steaming temperature. The results indicate that the stability of the catalyst without steam-treatment is low and the steaming leads to increasing the catalyst stability. Although the catalyst with smaller particle size has the lower light olefins selectivity, it is more stable in MTP. For the catalyst with larger particle size, the longer diffusion pathways for reactants and products lead to cracking of higher hydrocarbons and consequently increase potential of coke formation on the catalyst surface. Therefore, the activity of the catalyst with larger particle sizes was decrease after 160 h of time on stream and thereafter the heavy olefins which exit the reactor without cracking are increased.

Conclusion

In this study, the effect of steaming process on the catalyst structure and the performance of the MTP reaction was investigated. It was observed that the pore size and the pore volume of the catalyst are generally increased by steaming and the particle

size plays an important role in this context. The catalyst with larger particle size with smaller pores shows higher methanol conversion and therefore, it can be concluded that there is no limitation with regard to the accessibility of the reactants in the MTP system and the methanol conversion is controlled by the acidity of the catalyst. The amount of light olefins obtained for the catalyst with larger particle size is more than the ones achieved for the smaller size catalyst. This difference is attributed to the improved product shape selectivity of the catalyst and transforming the strong acidity of the surface catalyst to the weak one. The occurring change in the structure of the larger particle size causes a change in the diffusion characteristics of the catalyst by decreasing its pore dimensions and openings. This leads to longer diffusion pathways for reactants and products, which might facilitate multiple methylations and consequently cracking of higher hydrocarbons before exiting the catalyst. As a result, the amounts of light olefins, unlike the higher ones, are reduced in this case.

Acknowledgements This work was funded by the Iran's Ministry of Science, Research and Technology (Grant No. 8563214-03). The authors thank Dr. Frank Rosowski, Julia Bauer and Christian Schulz (Uni-Cat BASF Joint Lab) for their help in TPD experiments, and Mohammad Ali Khadivi (dbta, TU Berlin) for BET measurements.

References

1. Haag S, Rothaemel M, Lin L, Castillo-Welter F, Gorny M (2015) Methanol to propylene: a proven technology for on-purpose propylene production, Dresden
2. Hadi N, Niaei A, Nabavi SR, Alizadeh R, Shirazi MN, Izadkhah B (2016) An intelligent approach to design and optimization of M-Mn/H-ZSM-5 (M: Ce, Cr, Fe, Ni) catalysts in conversion of methanol to propylene. J Taiwan Inst Chem Eng 59:173–185
3. Rashidi H, Shariati A, Khosravi-Nikou MR, Hamoule T (2016) A selective catalyst for methanol conversion into light olefin with a high propylene to ethylene ratio. Korean J Chem Eng 33:2319–2324
4. Ahmed S (2012) Methanol to olefins conversion over metal containing MFI-type zeolites. J Porous Mater 19:111–117
5. Bai T, Zhang X, Liu X, Chen T, Fan W (2016) Coupling conversion of methanol and 1-butylene to propylene on HZSM-5 molecular sieve catalysts prepared by different methods. Korean J Chem Eng 33:2097–2106
6. Kim HG, Lee KY, Jang H-G, Song YS, Seo G (2010) Simulation of methanol-to-olefin reaction over SAPO-34 catalysts with different particle sizes: formation of active sites and deactivation. Korean J Chem Eng 27:1773–1779
7. van der Bij HE, Weckhuysen BM (2015) Phosphorus promotion and poisoning in zeolite-based materials: synthesis, characterisation and catalysis. Chem Soc Rev 44:7406–7428
8. Dorado F, Romero R, Cañizares P (2002) Hydroisomerization of *n*-butane over Pd/HZSM-5 and Pd/Hβ with and without binder. Appl Catal A 236:235–243
9. Zhou J, Teng J, Ren L, Wang Y, Liu Z, Liu W, Yang W, Xie Z (2016) Full-crystalline hierarchical monolithic ZSM-5 zeolites as superiorly active and long-lived practical catalysts in methanol-to-hydrocarbons reaction. J Catal 340:166–176
10. Lange J-P, Mesters CMAM (2001) Mass transport limitations in zeolite catalysts: the dehydration of 1-phenyl-ethanol to styrene. Appl Catal A 210:247–255
11. Olsbye U, Svelle S, Bjørgen M, Beato P, Janssens TVW, Joensen F, Bordiga S, Lillerud KP (2012) Conversion of methanol to hydrocarbons: how zeolite cavity and pore size controls product selectivity. Angew Chem Int Ed 51:5810–5831
12. Jabbari A, Abbasi A, Zargarnezhad H, Riazifar M (2017) A study on the effect of SiO2/Al2O3 ratio on the structure and performance of nano-sized ZSM-5 in methanol to propylene conversion. Reac Kinet Mech Cat 121:763–772

13. Ghalbi-Ahangari M, Ranjbar PR, Rashidi A, Teymuri M (2017) The high selectivity of Ce-hierarchical SAPO-34 nanocatalyst for the methanol to propylene conversion process. Reac Kinet Mech Cat 122:1265–1279
14. Liu J, Zhang C, Shen Z, Hua W, Tang Y, Shen W, Yue Y, Xu H (2009) Methanol to propylene: effect of phosphorus on a high silica HZSM-5 catalyst. Catal Commun 10:1506–1509
15. Dehertog WJH, Froment GF (1991) Production of light alkenes from methanol on ZSM-5 catalysts. Appl Catal 71:153–165
16. Lee K-Y, Lee H-K, Ihm S-K (2010) Influence of catalyst binders on the acidity and catalytic performance of HZSM-5 zeolites for methanol-to-propylene (MTP) process: single and binary binder system. Top Catal 53:247–253
17. Zhuang J, Ma D, Yang G, Yan Z, Liu X, Liu X, Han X, Bao X, Xie P, Liu Z (2004) Solid-state MAS NMR studies on the hydrothermal stability of the zeolite catalysts for residual oil selective catalytic cracking. J Catal 228:234–242
18. Lee Y-J, Kim JM, Bae JW, Shin C-H, Jun K-W (2009) Phosphorus induced hydrothermal stability and enhanced catalytic activity of ZSM-5 in methanol to DME conversion. Fuel 88:1915–1921
19. Lischke G, Eckelt R, Jerschkewitz HG, Parlitz B, Schreier E, Storek W, Zibrowius B, Öhlmann G (1991) Spectroscopic and physicochemical characterization of P-modified H-ZSM-5. J Catal 132:229–243
20. Tanco M, Viles E (2009) Pozueta L. In: Ao S-I, Gelman L (eds) Comparing different approaches for design of experiments (DoE). Springer, Dordrecht, pp 611–621
21. Rahmani M, Taghizadeh M (2017) Synthesis optimization of mesoporous ZSM-5 through desilication-reassembly in the methanol-to-propylene reaction. Reac Kinet Mech Cat 122:409–432
22. Zhu Z, Lu G, Zhang Z, Guo Y, Guo Y, Wang Y (2013) Highly active and stable Co3O4/ZSM-5 catalyst for propane oxidation: effect of the preparation method. ACS Catal 3:1154–1164
23. Lee Y-J, Kim Y-W, Viswanadham N, Jun K-W, Bae JW (2010) Novel aluminophosphate (AlPO) bound ZSM-5 extrudates with improved catalytic properties for methanol to propylene (MTP) reaction. Appl Catal A 374:18–25
24. Tan IAW, Ahmad AL, Hameed BH (2008) Optimization of preparation conditions for activated carbons from coconut husk using response surface methodology. Chem Eng J 137:462–470
25. Garg UK, Kaur MP, Garg VK, Sud D (2008) Removal of Nickel(II) from aqueous solution by adsorption on agricultural waste biomass using a response surface methodological approach. Biores Technol 99:1325–1331
26. Myers RH, Montgomery DC, Anderson-Cook CM (2009) Response surface methodology: process and product optimization using designed experiments, Wiley
27. Almutairi SMT, Mezari B, Pidko EA, Magusin PCMM, Hensen EJM (2013) Influence of steaming on the acidity and the methanol conversion reaction of HZSM-5 zeolite. J Catal 307:194–203
28. Xin H, Li X, Fang Y, Yi X, Hu W, Chu Y, Zhang F, Zheng A, Zhang H, Li X (2014) Catalytic dehydration of ethanol over post-treated ZSM-5 zeolites. J Catal 312:204–215
29. Caeiro G, Magnoux P, Lopes JM, Ribeiro FR, Menezes SMC, Costa AF, Cerqueira HS (2006) Stabilization effect of phosphorus on steamed H-MFI zeolites. Appl Catal A 314:160–171
30. Blasco T, Corma A, Martínez-Triguero J (2006) Hydrothermal stabilization of ZSM-5 catalytic-cracking additives by phosphorus addition. J Catal 237:267–277
31. van der Bij HE, Aramburo LR, Arstad B, Dynes JJ, Wang J, Weckhuysen BM (2014) Phosphatation of zeolite H-ZSM-5: a combined microscopy and spectroscopy study. ChemPhysChem 15:283–292
32. van der Bij HE, Cicmil D, Wang J, Meirer F, de Groot FMF, Weckhuysen BM (2014) Aluminum-phosphate binder formation in zeolites as probed with X-ray absorption microscopy. J Am Chem Soc 136:17774–17787
33. Zhao G, Teng J, Xie Z, Jin W, Yang W, Chen Q, Tang Y (2007) Effect of phosphorus on HZSM-5 catalyst for C4-olefin cracking reactions to produce propylene. J Catal 248:29–37
34. Cardoso MJB, Rosas DDO, Lau LY (2005) Surface P and Al distribution in P-modified ZSM-5 zeolites. Adsorption 11:577–580
35. Cao J, Wu Y, Jin Y, Yilihan P, Huang W (2014) Response surface methodology approach for optimization of the removal of chromium(VI) by NH2-MCM-41. J Taiwan Inst Chem Eng 45:860–868
36. Hemelsoet K, Van der Mynsbrugge J, De Wispelaere K, Waroquier M, Van Speybroeck V (2013) Unraveling the reaction mechanisms governing methanol-to-olefins catalysis by theory and experiment. ChemPhysChem 14:1526–1545
37. Li Z, Martínez-Triguero J, Yu J, Corma A (2015) Conversion of methanol to olefins: stabilization of nanosized SAPO-34 by hydrothermal treatment. J Catal 329:379–388

38. Sun X, Mueller S, Shi H, Haller GL, Sanchez-Sanchez M, van Veen AC, Lercher JA (2014) On the impact of co-feeding aromatics and olefins for the methanol-to-olefins reaction on HZSM-5. J Catal 314:21–31
39. Chang CD, Chu CTW, Socha RF (1984) Methanol conversion to olefins over ZSM-5. J Catal 86:289–296
40. Sugimoto M, Katsuno H, Takatsu K, Kawata N (1987) Correlation between the crystal size and catalytic properties of ZSM-5 zeolites. Zeolites 7:503–507
41. Rownaghi AA, Rezaei F, Hedlund J (2011) Yield of gasoline-range hydrocarbons as a function of uniform ZSM-5 crystal size. Catal Commun 14:37–41
42. Rownaghi AA, Hedlund J (2011) Methanol to gasoline-range hydrocarbons: influence of nanocrystal size and mesoporosity on catalytic performance and product distribution of ZSM-5. Ind Eng Chem Res 50:11872–11878
43. Choi M, Na K, Kim J, Sakamoto Y, Terasaki O, Ryoo R (2009) Stable single-unit-cell nanosheets of zeolite MFI as active and long-lived catalysts. Nature 461:246–249
44. Khare R, Millar D, Bhan A (2015) A mechanistic basis for the effects of crystallite size on light olefin selectivity in methanol-to-hydrocarbons conversion on MFI. J Catal 321:23–31
45. Kaeding WW, Chu C, Young LB, Butter SA (1981) Shape-selective reactions with zeolite catalysts. J Catal 69:392–398
46. Kaeding WW, Chu C, Young LB, Weinstein B, Butter SA (1981) Selective alkylation of toluene with methanol to produce para-Xylene. J Catal 67:159–174

Affiliations

Abolfazl Gharibi Kharaji[1,2] · Masoud Beheshti[1,3] · Jens-Uwe Repke[2] · Shahram Tangestani-nejad[4] · Oliver Görke[5] · Hamid Reza Godini[2]

[1] Department of Chemical Engineering, University of Isfahan, Hezarjirib Street, Isfahan, Iran

[2] Process Dynamics and Operation, Technische Universität Berlin, Strasse des 17. Juni 135, Sekr. KWT-9, 10623 Berlin, Germany

[3] Process Engineering Institute, University of Isfahan, Isfahan, Iran

[4] Department of Chemistry, University of Isfahan, Hezarjirib Street, Isfahan, Iran

[5] Department of Ceramic Materials, Institute for Material Science and Technologies, Technische Universität Berlin, Hardenberg straße 40, 10623 Berlin, Germany